Research Article Vol. 9, No. 10 / 1 October 2019 / Optical Materials Express 3925
Optical Materials EXPRESS

Hydrogels for targeted waveguiding and light diffusion

SONJA JOHANNSMEIER,[1,4,*] MARIA L. TORRES-MAPA,[2,4] DANIELE DIPRESA,[3,4] TAMMO RIPKEN,[1,4] DAG HEINEMANN,[1,4] AND ALEXANDER HEISTERKAMP[1,2,4]

[1] *Industrial and Biomedical Optics Department, Laser Zentrum Hannover e.V., Hollerithallee 8, 30419 Hannover, Germany*
[2] *Institute of Quantum Optics, Gottfried Wilhelm Leibniz Universität Hannover, Welfengarten 1, 30167 Hannover, Germany*
[3] *Lower Saxony Centre for Biomedical Engineering, Implant Research and Development, Department of Cardiothoracic, Transplantation and Vascular Surgery, Hannover Medical School, Stadtfelddamm 34, 30625 Hannover, Germany*
[4] *Lower Saxony Centre for Biomedical Engineering, Implant Research and Development, Stadtfelddamm 34, 30625 Hannover, Germany*
[*] *s.johannsmeier@lzh.de*

Abstract: Advances in photomedicine and optogenetics have defined the problem of efficient light delivery *in vivo*. Recently, hydrogels have been proposed as alternatives to glass or polymer fibers. These materials provide remarkable versatility, biocompatibility and easy fabrication protocols. Here, we investigate the usability of waveguides from poly(ethylene glycol) dimethacrylate for targeted light delivery and diffusion. Different hydrogel compositions were characterized with regard to water content, chemical stability, elasticity, refractive index and optical losses. Differences in refractive index were introduced to achieve targeted light delivery, and scattering polystyrene particles were dispersed in the hydrogel samples to diffuse the incident light. Complex constructs were produced to demonstrate the versatility of hydrogel waveguides.

1. Introduction

Several applications with therapeutic potential require deep tissue illumination. The growing field of optogenetics has been suggesting new treatment options for several conditions such as heart arrhythmias, laryngeal paralysis or neurological disorders [1–4]. Photodynamic therapy and biomodulation offer innovative treatment options for tumor removal and wound healing [5,6]. If the treatment targets are not located on or directly underneath the skin surface, long-term therapy would require reliable, biocompatible means of light delivery with minimal or no adverse effects. Current efforts to meet this increasing need mostly concentrate on the development of biocompatible fibers and micro-LEDs [7,8]. These devices can be manufactured to be stable and biocompatible but are difficult to integrate in a living system without causing any harm to the surrounding tissues. Alternatively, waveguiding fibers with favorable optical properties can be fabricated from hydrogel materials [9–11]. These fibers are soft and flexible and can be integrated into sensitive environments without inflicting injuries on the tissue. Hydrogels from natural or synthetic sources can be easily manufactured in the desired form using molds, masks and photolithography [12] or 3D printing [13,14]. Different materials and compositions can be combined to tune the hydrogel's characteristics and achieve advantageous properties such as toughness or elasticity [11,14,15]. Therefore, these materials present an interesting alternative for specialized biomedical applications, where geometry and properties of the waveguide need to be adjusted to the respective circumstances. While optical fibers have already been developed from different materials, these waveguides are only suitable for applications that require selective

#369574 https://doi.org/10.1364/OME.9.003925
Journal © 2019 Received 18 Jun 2019; revised 23 Aug 2019; accepted 23 Aug 2019; published 3 Sep 2019

Optical Materials EXPRESS

illumination of a small target area. Some methods, like the optogenetic control of larger muscles, would demand simultaneous stimulation of a large tissue area with patient-specific geometries and properties. Through careful selection of composition and additives, a hydrogel construct could include parts for controlled waveguiding and scattering in a single unit. Here, we investigate the suitability of chemically cross-linked poly(ethylene glycol) diacrylate (PEGDA) and dimethacrylate (PEGDMA) as optical waveguides and diffusors. PEGDMA hydrogels are biocompatible and bioinert [16] and have been used for waveguiding before [10,17]. In this study, we aim to extend the usability of PEGD(M)A hydrogels beyond simple waveguiding and evaluate their use as diffusors and compounds for targeted illumination. The material can be modified to increase bioactivity by encapsulating biological factors [18] or introducing attachment sites for cells [19,20]. We present an analysis of the optical properties of PEGD(M)A hydrogels from long polymer chains (700, 8000, 20000 Da) and provide insights into the hydrogel architecture. Scattering nano- and microparticles were used to achieve light diffusion, and different hydrogel compositions and geometries were tested for controlled waveguiding. In conclusion, we present a method for the production of versatile biocompatible waveguides that can be tuned to yield both selective and broad illumination and thereby fulfill the needs of specialized applications in photomedicine or optogenetics.

2. Methods

2.1. Hydrogel fabrication

Hydrogels were fabricated from poly(ethylene glycol) diacrylate (PEGDA, 700 Da, viscous liquid; Sigma Aldrich, USA) or dimethacrylate (PEGDMA, 8000 or 20000 Da, solid; both Polysciences Inc., USA). The hydrogel precursor was mixed with water at the desired weight concentration and allowed to dissolve completely. Then, ammonium persulfate (10% w/v in water) and TEMED (both Merck, Germany) were mixed into the solution at final concentrations of 1% and 0.1%, respectively. Solutions were immediately pipetted into molds and placed in a nitrogen-flooded box to avoid oxygen exposure during polymerization. Gels were allowed to form for 45-60 minutes to ensure complete polymerization and then stored in desalinated water for at least one day before further use. Molds were produced from PDMS-imprints (Sylgard 184, Dow Corning, USA) of 3D-printed forms, or from aluminum blocks with custom-made notches. For cylindrical hydrogels, silicone hoses with 2 mm diameter were used. The hoses were slit lengthwise to facilitate filling with the hydrogel precursor. Where applicable, polystyrene (PS; 0.625, 1 and 10 µm diameter, Kisker Biotech, Germany) or titanium dioxide (rutile, <5 µm, Sigma Aldrich) particles were mixed into the solutions before polymerization to increase scatter inside the hydrogels. Concentrations of PS-particles are indicated in the results section and were chosen to provide roughly the same number of particles for the different diameters. The mass ratio of TiO_2-particles to PEGDMA was 1:1, resulting in hydrogels saturated with TiO_2 particles. Compound hydrogels were produced layer by layer: After polymerization of the first part, the second part was added as a liquid precursor solution. The different components were covalently connected during the polymerization reaction. Cylindrical hydrogels with a concentration gradient of PS-particles were produced by pipetting one concentration after another into an upright silicone hose, avoiding gaps between or mixing of the layers. Hydrogel wedges were produced by first fabricating a particle-free hydrogel cube ($6 \times 8 \times 3$ mm), cutting through it diagonally and removing the upper half. The form was then refilled with a particle-containing precursor that polymerized on top of the first gel, resulting in one hydrogel block consisting of two wedges, one with and one without particles (see Fig. 8(m)).

Optical Materials EXPRESS

2.2. Material characterization

Elasticity of PEGDMA hydrogels (8000 Da 10% and 20000 Da 10%) was quantified with a tensile testing apparatus (Instron 5967 Dual Column Series, Instron, USA). Dumbbell-shaped hydrogels were secured between the clamps with sandpaper and stretch to failure was performed using a 100 N load cell. Six samples per material were tested to obtain the Young's modulus of elasticity.

Mass swelling ratios were determined for different hydrogel compositions with and without particles and at different pH-values. To assess the influence of the surrounding's pH value, samples were stored in water at pH = 4, 7 or 10, adjusted with HCl or NaOH, for 1 or 14 days. Solutions were renewed every 3-4 days. The wet weight was determined with a precision scale. Samples were then vacuum-dried for approx. 20 hours and weighed again. The mass swelling ratio was calculated as

$$Q_m = \frac{w_s - w_d}{w_d} \tag{1}$$

where w_s and w_d are the hydrogel weights in swollen and dried state, respectively. Q_m describes the weight increase of the completely swollen hydrogel. Three samples per composition and condition were tested and averaged.

2.3. Optical characterization

Refractive index measurements of hydrogels were performed with a swept source OCT system (central wavelength: 1325 nm, spectral bandwidth: 100 nm; Thorlabs, USA). The refractive index was calculated as the ratio of measured optical thickness and actual thickness. Three B-scans (3 × 3 mm) per sample were performed and averaged, and three samples per hydrogel composition were measured to obtain the refractive index.

Transmission and reflection measurements including the respective scatter were performed in a Lambda 900 spectrophotometer (PerkinElmer, USA) with an integrating sphere. Hydrogel discs were produced as described above in round aluminum molds with a diameter of 22 mm and height of 1 mm and stored in water for at least 24 hours before measurement. Thickness did not increase measurably during this time. Table 1 summarizes the tested samples.

Table 1. Hydrogel compositions measured with spectrophotometer

Hydrogel	Particles
700 10% / 25% / 50%	none
8000 10% / 25% / 50%	none
20000 10% / 25% / 50%	none
8000 10%	0.625 µm PS (1 mg/mL)
8000 10%	1 µm PS (2 mg/mL)
8000 10%	10 µm PS (20 mg/mL)
8000 10%	TiO_2 (saturated)

Wavescans between 250 nm and 1000 nm were performed in 1 nm steps at 500 nm/min in transmission and reflection mode. Three samples per composition were measured and averaged. Losses in percent were calculated from the measurement data as

$$\text{loss} = 100\% - \text{transmission}(\%) - \text{reflection}(\%) \tag{2}$$

Attenuation coefficients (dB/cm) were calculated at 450 nm:

$$\alpha = (10 * \log_{10} \frac{P(0)}{P(z)})/z \tag{3}$$

Optical Materials EXPRESS

where *P(0)* and *P(z)* are input power and power after a sample thickness of z cm. Power is given in relative terms, with input power = 100%. For samples containing polystyrene particles, averaged values were normalized to the respective maximum for each particle diameter to avoid biases due to different particle size and concentration. The resulting values can only be compared qualitatively. Measurements of attenuation coefficients were reproduced with a cut-back method for PEGDMA 8000 10% and 20000 10% at 450 nm. Hydrogels were produced in a 30 mm long silicone hose (diameter 2 mm). Irregular endings were trimmed with a scalpel. A glass fiber (200 µm core diameter, NA = 0.22) was inserted into the center of one end of the hydrogel cylinder. The sample was held upright above a photodiode to measure output power (P_{out}). Then, 1 cm of the gel was cut off and the measurement was repeated to obtain P_{in}. Eight samples of PEGDMA 8000 10% and six samples of PEGDMA 20000 10% were measured and averaged.

2.4. Characterization of light distribution

To assess the distribution of light within a hydrogel construct, flat (3 mm high) cuboids were fabricated and placed under a CMOS camera (Thorlabs) to visualize the path of the light and the effective brightness of the hydrogel surface. Different hydrogel designs are described in the results section. Light from a 450 nm laser diode (max. output 40 mW; Roithner Lasertechnik, Austria) was coupled into a glass fiber (200 µm core diameter, NA = 0.22; LifePhotonic, Germany) which was inserted into the side of the hydrogel. A half-wave plate and polarizing beam splitter were used to control output power at the fiber tip. For imaging, power was set to 250-300 µW. Two lenses (f = 35 mm and 125 or 75 mm; Thorlabs) were used to project the image on the CMOS chip and to adjust magnification.

Particle distribution over time was assessed with a confocal laser scanning microscope (Leica TCS SP5; Leica Microsystems, Germany). Four samples of PEGDMA 8000 10%, each < 1 mm thick, two containing 1 µm (1 mg/mL) and two containing 10 µm PS-particles (10 mg/mL) were imaged immediately after production and again after 1, 5, 7, 14 and 28 days. Samples were stored in demineralized water between experiments. Stacks were recorded with a transmission PMT, using the 633 nm HeNe laser for illumination.

2.5. Data analysis

Data analysis and visualization was performed with R (v3.3.3 [21–23]). For the multiple linear regression model, the non-constant variance test was used to check for homoscedasticity, and the variance inflation factor was calculated to test for multicollinearity. Other assumptions (linear relationship, normal distribution of residuals) were checked with diagnostic plots. Image analysis was done with ImageJ/FIJI (v2.0.0 [24]). To calculate the distance between particles in hydrogel samples, individual slices from stacks were converted to binary images with manual thresholding after background subtraction. A plugin [25] was used to calculate the distance to the nearest neighbor for each particle on two slices per sample at time points 0 and 28 days. Values were pooled for each particle size and time point, and mean and standard deviation were calculated.

3. Results

3.1. Material characteristics

Results for mass swelling ratios of hydrogels without particles showed that at pH = 7, the water content depended on the polymer's chain length and concentration (Fig. 1(a)). Water content increased with chain length and decreased with increasing polymer concentration. While PEGDA 700 50% only absorbed water a little more than its dry weight, water content increased to 14 times the gel's dry weight for PEGDMA 20000 10%. A multiple linear regression model was fitted to describe the observed data. The influence of both chain length and concentration on the hydrogel's mass swelling ratio was highly significant ($p = 9.48*10^{-12}$ and $1.077*10^{-9}$,

Optical Materials EXPRESS

respectively). Together, these two variables accounted for 89.7% of the observed variability (adjusted $R^2 = 0.8968$).

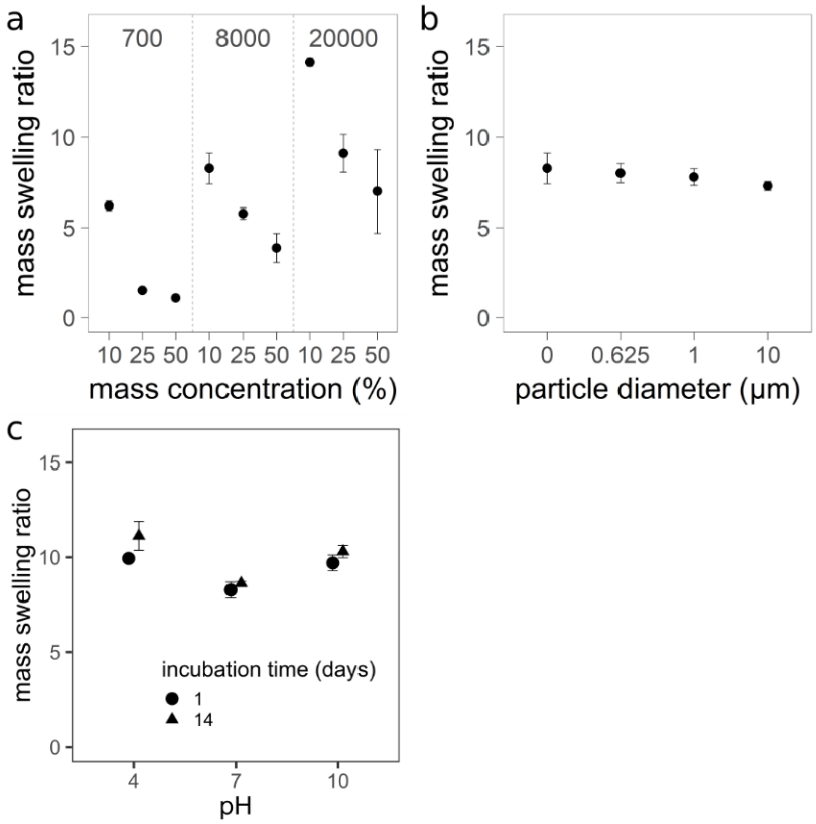

Fig. 1. Mass swelling ratio of PEGD(M)A hydrogels of different compositions stored under various conditions. a: Effect of chain length and concentration. b: Effect of PS-particles with different diameters embedded in the hydrogels (PEGDMA 8000 10%). c: PEGDMA 8000 10% stored under different pH-conditions for 1 or 14 days. Data points show mean values ± standard deviation of three samples each (five samples for pH 4, 14 days).

Polystyrene particles with varying diameters were added to PEGDMA 8000 10% and the mass swelling ratio was determined again. Although the overall effect was smaller, particle size correlated negatively with mass swelling ratio ($p = 3.379*10^{-3}$, Fig. 1(b)), with an adjusted R^2 of 0.5526. Particle-free gels absorbed 1.134 times as much water, on average, as the same gels containing the largest particles.

Additionally, the influence of the medium's pH-value on PEGDMA 8000 10% was tested. Samples were stored at pH = 4, 7 or 10, respectively, for 1 or 14 days. Both high and low pH increased the mass swelling ratio during one day of incubation (Fig. 1(c)). After 14 days, the value of the sample stored at pH = 4 had increased to more than 12-fold its dry weight, which was almost 1.5 times as high as the value for pH = 7 after the same incubation time. The mass swelling ratio increased less strongly at pH = 10 within the 14 days. At neutral pH, the value increased only slightly, indicating that small amounts of water were still absorbed after more than one day.

Young's modulus of elasticity was measured for two hydrogel compositions. The first sample of PEGDMA 8000 10% broke in the clamped area and was excluded from the average. Young's

Optical Materials EXPRESS

moduli were determined at 334 ± 46 kPa (PEGDMA 8000 10%) and 60 ± 5 kPa (20000 10%), respectively. Other compositions were not quantified. Qualitatively, shorter polymer chains at higher concentrations yielded stiffer hydrogels. PEGDA 700 ≥ 50% could not be elastically deformed and snapped when bent.

The refractive index of different PEGD(M)A hydrogels was obtained via OCT measurement (Fig. 2). In general, the refractive index was positively correlated with polymer concentration and negatively correlated with chain length. Considering the results from mass swelling ratio measurements, a negative correlation between water content and refractive index was observed. Values for the refractive indices ranged from 1.343 (PEGMDA 20000 10%, mean) to 1.437 (PEGDA 700 90%, mean). The lower limit is the refractive index of water (1.33).

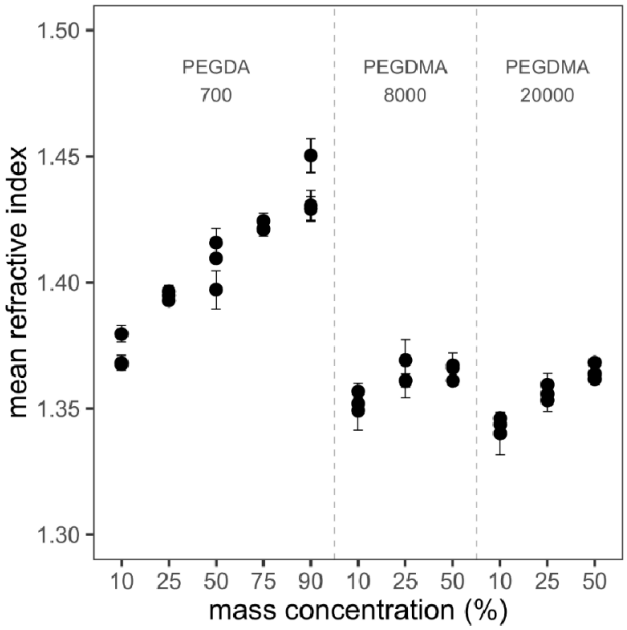

Fig. 2. Refractive index measurements of PEGD(M)A hydrogels of different compositions. Each data point represents the average of three measurements ± standard deviation for one sample. Three samples were measured for each composition.

Hydrogels from PEGDA 700 10% were not entirely transparent, yielding lower transmission values especially in the UV-A and visible range than PEGDA 700 with a higher concentration (Fig. 3(a)). About 10% of the non-transmitted light in the visible range was reflected by these samples, resulting in less than 10% loss for visible wavelengths. PEGDA 700 25% had the lowest losses overall but showed relatively strong reflection (Fig. 3(b)). For PEGDMA 8000, there were no clear distinctions between hydrogels with different polymer concentrations (Figs. 3(d)–3(f)), but losses were lowest for 25%. Transmission decreased with increasing concentration for PEGDMA 20,000 (Fig. 3(g)). There was a dip in transmission values around 450 nm that was most pronounced for 25%. Losses were lowest for 10%.

PS-particles of different sizes were introduced so that samples contained roughly the same particle number. Reflection ranged between 25 and 15% for most of the visible ratio, the values being largest for 0.625 µm-particles. Losses were low (approx. 5%) for 10 µm particles and ranged between 15 and 20% for the smaller particles. Measurements were qualitatively similar for particles with 0.625 and 1 µm diameter as well as for 10 µm and particle-free gels (Figs. 4(a)–4(c)). Despite the larger standard deviation of averaged reflection values of gels containing 10 µm or no

Optical Materials EXPRESS

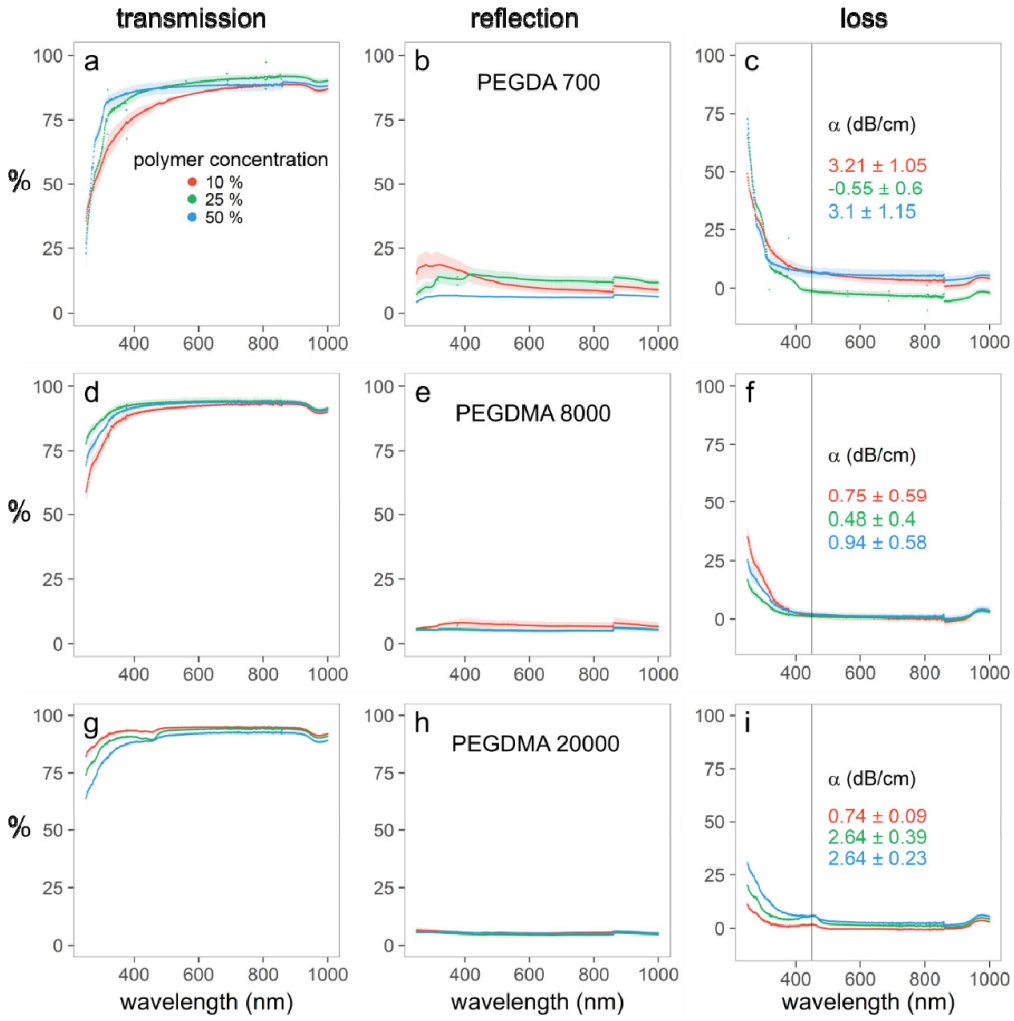

Fig. 3. Transmission and reflection measured for different hydrogel compositions. Losses and attenuation coefficients were calculated from the measurement data. a-c: PEGDA 700; d-f: PEGDMA 8000; g-i: PEGDMA 20000. At 860 nm, a detector change occurred in the spectrophotometer, resulting in small measurement artifacts. Negative loss values of PEGDA 700, 25% (c) should be regarded as statistical noise. Each data point represents the average of three samples ± standard deviation.

Optical Materials EXPRESS

particles, the individual curves all had a common shape (data not shown). Reflection of samples with small particles decreased with wavelength, and transmission increased more slowly. Losses of samples with 10 µm or without particles decreased stronger with respect to the maximum value (Fig. 4(c)).

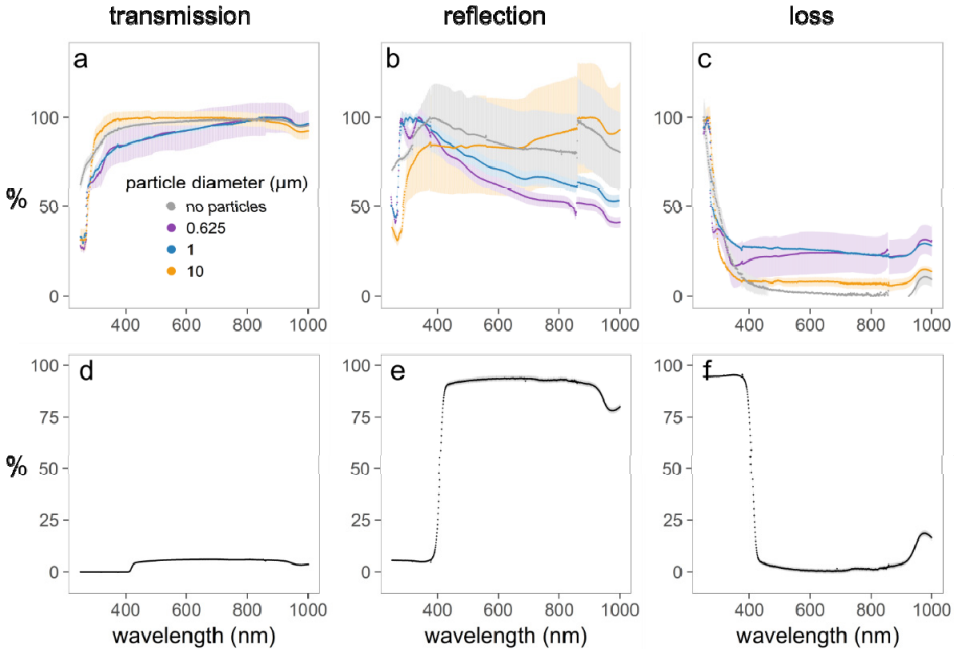

Fig. 4. a-c: Transmission, reflection and loss measurements of PEGDMA 8000 10% containing PS-particles, each curve normalized to its maximum value. Normalization inflated the standard deviations as well as the measurement artifacts at 860 nm (b, c). These artifacts originate from a detector change in the spectrophotometer. The curves can only be compared qualitatively. d-f: Transmission, reflection and losses for PEGDMA 8000 10% saturated with TiO_2-particles. Each data point represents the average of three samples ± standard deviation.

Hydrogels saturated with TiO_2 particles were not transmissive below 410 nm, and most of the light was absorbed in this range (Figs. 4(d)–4(f)). Between approx. 420 and 960 nm, at least 80% of the incoming light was reflected. This proportion rose to at least 90% between 430 and 915 nm. Losses were mostly below 5% in that range.

To complement the results from transmission measurements, cut-back measurements were performed on cylindrical hydrogel samples from PEGDMA 8000 10% and 20000 10%. The resulting attenuation coefficients at 450 nm were 0.80 ± 0.22 dB/cm and 0.80 ± 0.27 dB/cm, respectively. These values are in good agreement with those obtained from spectrophotometer measurements, although with this method, light that might have been coupled out of the hydrogel laterally could not be quantified.

3.2. *Light distribution and diffusion*

The long-term stability of particle suspensions within the hydrogel was evaluated over the course of four weeks in thin PEGDMA 8000 10% samples containing 1 µm or 10 µm PS-particles. No conspicuous changes were observed in any of the samples (Fig. 5). Specifically, no changes were detected in the average distance between neighboring particles (Table 2), suggesting that particle distribution remained stable. Occasionally, clusters of 10 µm particles were observed at the very

Optical Materials EXPRESS

bottom of a sample (Figs. 5(g) and 5(h)). Formation of these clusters was not time dependent but occurred before the first imaging time point, presumably during sample production. Clusters of 10 µm particles could be observed in both samples at all time points, but were never larger than approx. 100 particles.

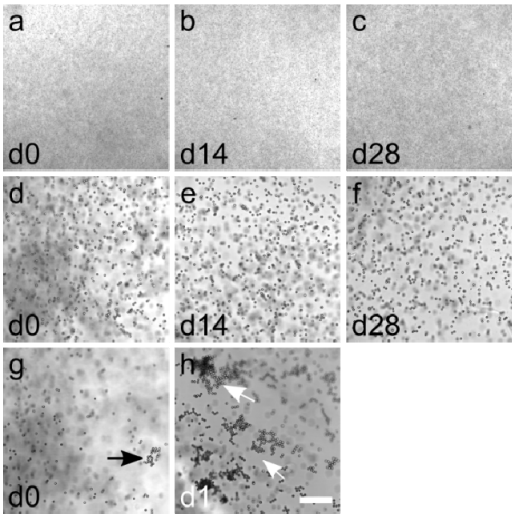

Fig. 5. Confocal images of PS-particles in PEGDMA-hydrogels at different time points after sample production. a-c: PS-particles with 1 µm diameter. d-h: PS-particles with 10 µm diameter. Occasionally, 10 µm particles formed clusters in the bottom layer of a hydrogel (g-h, arrows). Scale bar 150 µm for all images.

Table 2. Mean distances between neighboring particles in PEGDMA 8000 10% after 1 and 28 days of incubation in water.

Particle diameter (µm)	Incubation time (days)	Distance to nearest neighbor (µm, mean ± standard deviation)
1 (1 mg/mL)	1	5.2 ± 1.7
1 (1 mg/mL)	28	4.1 ± 1.9
10 (10 mg/mL)	1	21.4 ± 11.2
10 (10 mg/mL)	28	23.1 ± 11.4

Light distribution on the hydrogel surface was assessed with a CMOS camera mounted perpendicularly to the direction of light propagation. The influence of size and concentration of the scattering polystyrene particles is shown in Fig. 6.

In hydrogels containing no particles, light from the fiber propagated on a cone-shaped path to the opposite end, only visible from above at high exposure times (Figs. 6(b) and 6(c)). Homogeneously distributed scattering particles with 0.625, 1 or 10 µm diameter improved waveguiding towards the sample surface. At higher concentrations, light was predominantly scattered at the fiber tip. Intensity decreased in all directions with increasing distance to the fiber. Generally, the scattering cone formed by larger particles was directed more towards the forward direction, with more light reaching the opposite ending (Fig. 6(j), arrowhead), as would have been expected in accordance with Mie theory. There were no substantial differences in illumination efficiency of the individual mixtures given a sufficiently high particle concentration. At low concentrations, larger particles showed better scattering properties.

To improve light output at the sample surface, the fiber was replaced with a polymer optical fiber with a roughened surface in its final segment (4 cm; LifePhotonic). Light radiated in all

Optical Materials EXPRESS

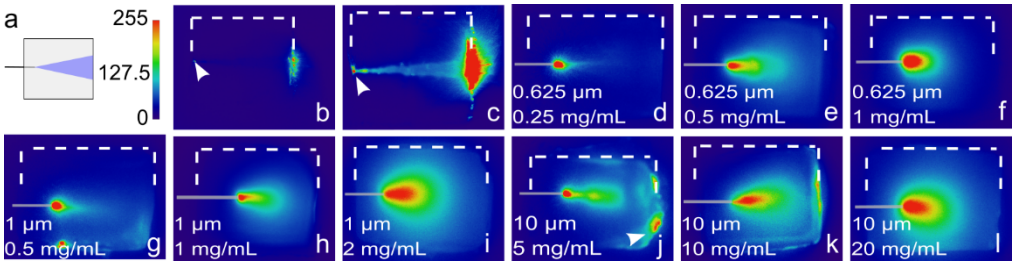

Fig. 6. Pseudocolor images of light distribution within PEGDMA 8000 10%, imaged from above. The color scale is shown in a and is the same for all pseudocolor images in this work. Numbers indicate the corresponding gray value. The glass fiber was inserted from the left and is indicated as a grey line. Dashed white lines mark the dimensions of the samples. a: Schema of sample setup. Light output from the surface was imaged perpendicularly from above. b,c: particle-free gel. The path of light distribution from the fiber ending (arrowheads) is clearly visible at an exposure time of 5 ms (c), but not 1 ms (b). d-l: Particle diameter and concentration are given in the images. The arrowhead in j marks light exiting the sample after being scattered in forward direction from the fiber tip. All images were taken with an exposure time of 0.05 ms. Samples in b,c are 10×10 mm, all others are 6×8 mm.

directions from this fiber segment. In hydrogels containing scattering particles, light distribution was strongly enhanced by this illumination mode, although the largest proportion of light still radiated from the fiber tip (Fig. 7(c)). Increasing the number of fibers in one hydrogel yielded good illumination across almost the entire sample surface (Figs. 7(e) and 7(f)). In hydrogels without particles, light from the fiber reached the surface but was not distributed any further inside the gel (Figs. 7(g) and 7(h)).

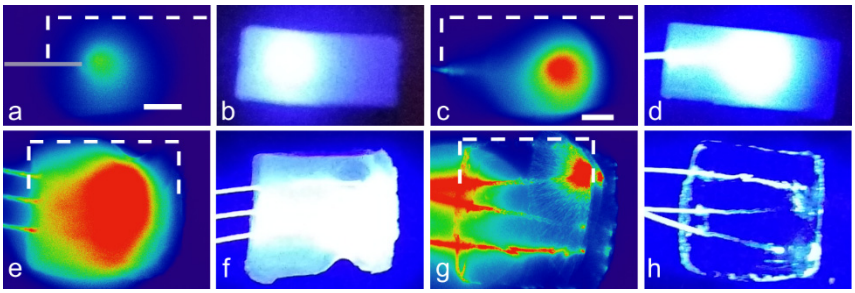

Fig. 7. Pseudocolor images and photographs of PEGDMA 8000 10% containing 2 mg/mL of 1 µm PS-particles (a-f) or no particles (g, h). Dashed white lines mark the sample borders, and the grey line (a) indicates the position of the fiber. a, b: The same fiber as in Fig. 6 was used for illumination. c, d: A polymer fiber with a roughened surface was used that radiated light from its final 4 cm segment. e-g: A bundle of three structured fibers was inserted into one sample. Samples in a-d are 10×20 mm (scale bars 3 mm), samples in e-h are 10×10 mm. Exposure time (pseudocolor images) was 0.1 ms.

A reflective hydrogel layer containing highly concentrated TiO_2 particles was introduced to enhance scattering towards the sample surface and shield the bottom side against losses. These hydrogels showed >90% reflection at 450 nm (see Fig. 4(e)). In samples containing polystyrene particles, such a reflective layer strongly increased the surface brightness across the whole sample (Figs. 8(c) and 8(k)). Reflections on the bottom side could be seen in particle-free hydrogels with a TiO_2-layer (Figs. 8(b) and 8(h)). The bottom surface of both samples appeared dark in the imaging setup, indicating that light output via this side was negligible. The reflecting layer could

Optical Materials EXPRESS

be used to direct the light to the surface at a desired location. To achieve an output at the surface, a hydrogel was produced that consisted of two wedges, one with and one without TiO_2-particles (see Fig. 8(m)). Most of the light was reflected at the sloped surface of the bottom gel and was visible at the surface in the middle of the sample (Figs. 8(n) and 8(o)).

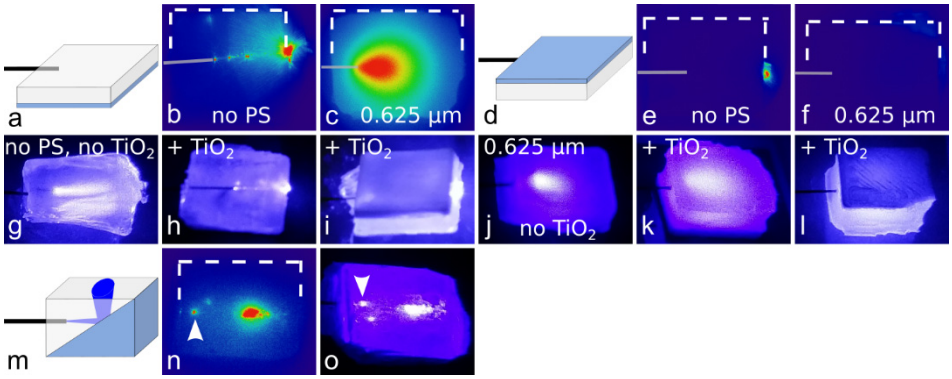

Fig. 8. Pseudocolor images and photographs of PEGDMA 8000 10% containing high concentrations of TiO_2 in the bottom layer. Grey lines indicate positioning of the fiber, and white dashed lines mark the hydrogel borders. a: Schema for sample setup in b,c. The TiO_2-layer is represented in blue. b: particle-free hydrogel with TiO_2-containing bottom layer, upper surface. c: Sample containing 1 mg/mL of 0.625 µm PS-particles, upper surface. d: Schema for sample setup in e,f. e,f: The same samples as in b,c, from below. Light exiting to the right is visible in the particle-free sample in e. g-i: particle-free samples with (h,i) and without (g) a reflective TiO_2-layer. j-l: Hydrogels with 1 mg/mL 0.625 PS-particles with (k,l) and without (j) a TiO_2-layer. m: Schema for sample in n,o. n,o: Sample from two hydrogel wedges, the bottom wedge containing TiO_2-particles. The arrowheads mark the fiber ending. Light reflected from the sloped TiO_2-layer is visible from above. All samples are 6×8 mm. Pseudocolor images were recorded with exposure times of 0.05 ms (c,f), 1 ms (b,e) or 0.1 ms (n).

Different compound constructs were evaluated to achieve controlled waveguiding in combination with light diffusion through scattering. A short straight hydrogel cylinder inside a second hydrogel block was tested to alter light distribution specifically at the fiber ending. Hydrogel material and scattering particles were changed to visualize the impact of these parameters. PEGDMA 8000 10% was chosen for the gel block, and the cylinder was made from either PEGDA 700 50% or PEGDMA 8000 10%. Overall, light distribution on a larger scale was not strongly influenced by the different strategies. Coupling the fiber into a particle-free cylinder transported the light further into the sample before it was scattered in the outer gel. Over short distances, this could be achieved with the same material (i.e. the same refractive index) for the cylinder and the outer gel (Figs. 9(f)–9(h)).

Using a material with higher refractive index for the cylinder generally directed the light further along the cylinder axis, occasionally resulting in reflections at the cylinder's borders. Light output into the surrounding gel was hindered in these samples (Figs. 9(b)–9(e)). As observed before (Fig. 6), combinations that included 1 µm PS-particles (2 mg/mL) in the outer block scattered the light further to the sides (not shown).

For a second test, the cylinder was replaced by a Y-shaped hydrogel made from PEGDA 700 50%. Depending on the illumination angle, the inner gel with a higher refractive index acted either as a shield or a guiding structure. Figures 10(a) and 10(d) show the Y-shaped gel containing the scattered light between its branches. When the light was coupled into the structure diagonally, it was scattered along the borders and at the end of the respective branch (Figs. 10(b) and 10(e)).

Optical Materials EXPRESS

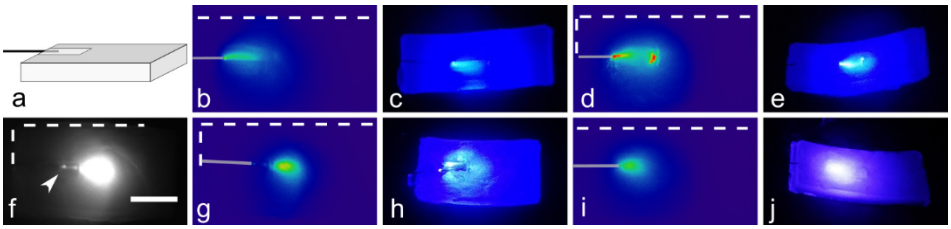

Fig. 9. a: Schema for compound samples in b-j, consisting of PEGDMA 8000 (10%) blocks containing 20 mg/mL of 10 µm PS-particles with a short cylindrical gel inside. Grey lines mark the fiber positions, and white dashed lines indicate the sample edges. b-e: cylinders from PEGDA 700 50%, without (b,c) or with (d,e) 20 mg/mL 10 µm PS-particles. f-j: The same samples with the cylindrical gel made from PEGDMA 8000 10%. The sample in f-h contains no particles in the inner cylinder. The arrowhead in f marks the fiber ending within the hydrogel cylinder. Scattering starts where the light enters the gel block containing PS-particles. Scale bar for f and pseudocolor images: 5 mm. All pseudocolor images where captured with an exposure time of 0.1 ms, the image in f was taken with an exposure time of 1 ms.

The effect of using compounds from materials with different refractive indices was clearly visible in a particle-free sample (Figs. 10(c) and 10(f)). Light that hit the border of the Y-shape was refracted back into the branch.

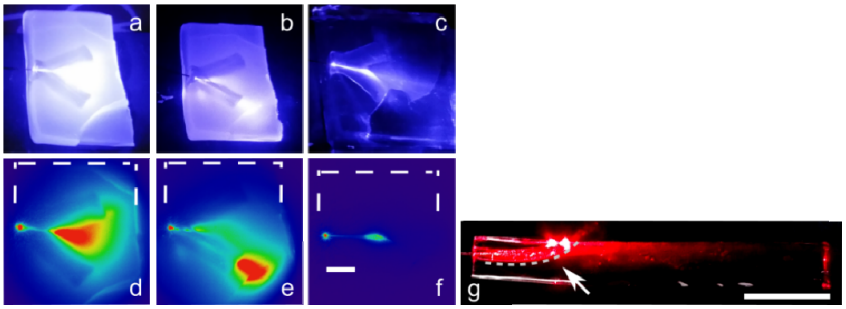

Fig. 10. Pseudocolor images and photographs of Y-shaped PEGDA 700 50% (particle-free) inside of PEGDMA 8000 10% containing 0.5 mg/mL of 0.625 µm PS-particles (a,b,d,e) or no particles (c,f). Illumination occurred from the left. Dashed white lines indicate the sample borders. a,d: Light coupled into the construct at 90° travelled straight into the PEGDMA-block. Scattered light was refracted back into the block by the branches of PEGDA 700. b,e: The fiber was tilted towards one of the branches. c,f: The same setup as in b,e with particle-free PEGDMA. Pseudocolor images were captured with an exposure time of 5 ms. Scale bar (d-f) 3 mm. g: PEGDMA 20000 20% block containing a longer, curved cylinder from PEGDA 700 20%, indicated by the dashed grey line. At the bend, light leaves the cylinder and propagates into the gel block (arrow). Bright spots at the top mark the exit site of the light travelling within the cylinder. Scale bar 10 mm.

A gel-in-gel construct was tested to guide the light into the hydrogel sample before distributing it to the surface. In Fig. 10(g), differences in refractive index values were chosen so that the incident light propagated within a core gel as long as it was not curved. At the bending of the core, light was coupled into the surrounding gel block.

The effect of a longitudinal particle concentration gradient was tested with long cylindric hydrogels (approx. 3 cm long, 2 mm diameter). Polystyrene particles were introduced to these samples with and without a concentration gradient. The sample with a concentration gradient

Optical Materials EXPRESS

was produced in three segments of approx. 1 cm length (30 µL volume), containing 1 µm-PS particles at concentrations of 0.25 mg/mL, 0.5 mg/mL and 1 mg/mL, respectively.

Two gels for comparison contained either 1 µm PS-particles at 1 mg/mL over the entire sample length or no particles at all. Light from the fiber travelled along the particle-free hydrogel cylinder to its opposite ending with little output to the sides (Figs. 11(a) and 11(b)). Introducing particles in a uniform concentration resulted in a bright section at the fiber tip and poor illumination of the rest of the cylinder (Figs. 11(c) and 11(d)). The cylinder with the particle gradient displayed strong improvement of downstream illumination (Figs. 11(e) and 11(f)).

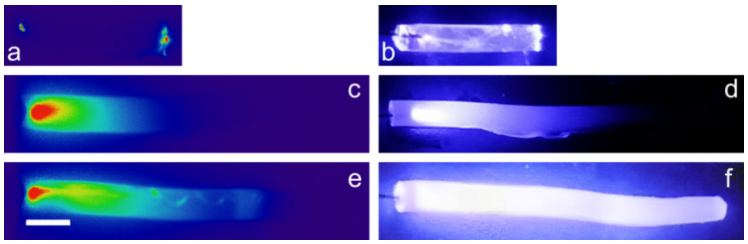

Fig. 11. Pseudocolor images and photographs of light coupled into PEGDMA 8000 (10%) cylinders containing no particles (a,b), evenly distributed 1 µm PS-particles (1 mg/mL; c,d) or ascending concentrations of 1 µm PS-particles (0.25/0.5/1 mg/mL; e,f). The fiber was inserted from the left. Pseudocolor images were captured with an exposure time of 1 ms. Scale bar (a,c,e) 3 mm. Samples in a,b were shorter (approx. 1 cm) than the others (approx. 3 cm).

4. Discussion

Measurements of the mass swelling ratio showed that, as expected, hydrogels consisting of loose networks absorbed the most water. Specifically, the samples made from the longest polymer chains at the lowest concentration yielded the highest value of 14.13 (see Fig. 1). This has been observed before, although values for swelling ratio have been reported to be higher [17,26,27]. Introducing water-dispersible microparticles to the network decreased its capacity for water retention, possibly due to adsorption of the hydrophobic PEG chains by polystyrene particles [28,29]. Hydrophobic interactions could tighten the polymer network, explaining the lower water content. Incubation at increased or decreased pH-values increased the mass swelling ratio over time. This indicates changes in the hydrogel's network architecture, since a looser network is associated with higher values. It has been shown before that the ester bonds in PEGDA hydrogels can be cleaved in high pH-environments, causing the polymers to fall apart within 3 days [16]. In our study however, we observed only a slight increase of water content after 14 days of incubation at pH = 10 and no disintegration of the samples. Long-term pH-stability is an important consideration for hydrogel implants, since the immune response to implant surfaces includes a pH decrease in order to degrade the foreign body [30].

Young's modulus of elasticity was lower for the hydrogels with a looser network (PEGDMA 20000 10%). The obtained values for Young's modulus are rather high compared with previously collected data [27,31,32]. Together with the low values for mass swelling ratios observed in this study, the data indicates that our hydrogels formed tighter polymer networks. PEGD(M)A hydrogels are often fabricated using a photoinitiator and UV light, with polymerization times between 1 and 15 minutes [17,26,27,31,32]. In this study, our chemically cross-linked hydrogels were allowed to polymerize for up to 60 minutes, although a physical gel was already formed after approx. 10 minutes. Removing the gel at an early time point usually left behind a small amount of unpolymerized liquid that would in turn continue to gel. It has been shown that

Optical Materials EXPRESS

hydrogels form tighter networks with increasing concentration of photoinitiator [33,34]. In our case, the combination of chemical crosslinking, concentration of polymerization starters and long polymerization time yielded particularly tight polymers. All these parameters can be adjusted to tune properties like water absorption and elasticity. However, the increased pH stability observed in our study suggests that incomplete polymerization reactions are conducted at the expense of physical integrity.

As expected, the hydrogel's refractive index decreases with increasing water content. The largest observed difference between a gel with high (20000 10%) and low (700 90%) water content was approx. 0.1 (see Fig. 2). Step-index fibers with a PEGDA core and alginate cladding have been realized with a refractive index step of roughly 0.14 [10], other step index hydrogel fibers were realized with an even smaller refractive index difference [11]. In our test structures, the refractive index difference between PEGDA 700 20% and PEGDMA 20000 20% was large enough to guide the light within the PEGDA 700 on a straight path. At the bend, light was coupled out (see Fig. 10(g)). Using the Y-shape from PEGDA 700 50% within PEGDMA 8000 10%, light was refracted on the inside or outside of the branches, guiding it towards the desired direction. A higher difference of refractive indices of the compounds would allow for light guiding in more complex geometries [10], whereas smaller differences can be used for coupling out of light at specific target structures, as shown in Fig. 10(g). It should be noted that refractive index differences between the waveguide and the surrounding medium must be kept in mind as well if the hydrogel is to be used with different tissues. All the modalities tested here were immersed in air. First imaging tests in water did not show any noticeable differences.

Short polymer chains at low concentrations (700 10% in our study) have a milky appearance. With increasing polymer concentration, samples become transparent. Optical losses within PEGDA 700 10% are still acceptable over short distances, making it interesting for structures were scattering is desired. In general, PEGD(M)A hydrogels display high transmission and low reflection in the visible and NIR range. PEGDMA 20000 displays a peak in loss values around 450 nm, a relevant wavelength for optogenetics. Losses in PEGDMA 20000 might also be increased because of streaks and irregularities that arose during sample production due to the poor solubility of large polymers in water. To achieve 50 wt.-% PEGDMA 20000, the polymer had to be dissolved for several hours or overnight. Still, these samples display good transmission. PEGDMA 8000 combines low losses (< 1% per mm in most of the visible range for 10% and 25% wt.-concentration), good sample manageability and sufficient elasticity and can be considered a favorable base material for an implantable optical waveguide.

Transmission and reflection of PS-particle containing samples is more wavelength dependent for small particles than for large ones (10 µm) or particle-free samples (see Figs. 4(a)–4(c)). These measurements are in accordance with Mie theory, showing stronger scatter for shorter wavelengths and decreasing wavelength dependency with increasing particle size. Our measurements indicate that PS-particles remain stably dispersed in the hydrogels for at least four weeks. Nevertheless, stability of the distribution needs to be tested before implantation under more realistic conditions considering mechanical stress and chemical environment.

Using homogeneously distributed scattering particles in combination with a single point source only illuminates a limited area of the sample surface. We present different strategies to improve light output perpendicular to the direction of the fiber. One possibility is to use one or more structured fibers instead of point sources (Fig. 7). This is an effective solution, but introducing multiple fibers in a confined area might compromise sample stability. A highly reflective bottom layer scatters light back into the sample towards the upper surface (Fig. 8). Reflections can also be used to create single spots on the sample surface. These spots can be controlled by varying slope and location of the reflecting layers as well as number and angle of light sources. Compound structures with and without scattering particles can be used to control the site of light scattering and the direction of light propagation (Figs. 9 and 10). A sophisticated sample design allows for

Optical Materials EXPRESS

targeting of specific areas with only one point source, as was demonstrated with the Y-shaped waveguide. However, stability of compound structures needs to be considered with respect to their application. The smaller the surface shared by two gel components, the weaker will be the bond. Longitudinal concentration gradients efficiently increase scattering with increasing distance from the light source (Fig. 11). These gradients need to be introduced segment by segment in PEGDMA because the hydrogel precursor is liquid. In a more viscous material, it should be possible to produce gels in one piece, yielding a more homogeneous gradient and eliminating potential breaking points in the sample. Refractive index and compound structures can be exploited as a tool to control light distribution within a hydrogel construct. Depending on the material, modern 3D-printing techniques might be able to provide structures that direct the incident light to multiple sites of interest, introducing scatter as needed, all within one block of material and without the need for single fragile fibers.

5. Conclusion

Hydrogel waveguides from PEGD(M)A present versatile alternatives to glass fibers or microLEDs. Compound structures can be fabricated in a layer-by-layer design, controlling direction and scatter of the light. Low losses, biocompatibility, ease of production and handling and high tunability of material properties provide an excellent basis for the production of waveguides for specialized *in vivo* applications. Implants from these materials could be applied for long term PDT or optogenetics.

Funding

Bundesministerium für Bildung und Forschung (13N14085); Deutsche Forschungsgemeinschaft (EXC 1077/1).

References

1. T. Bruegmann, T. van Bremen, C. C. Vogt, T. Send, B. K. Fleischmann, and P. Sasse, "Optogenetic control of contractile function in skeletal muscle," Nat. Commun. **6**(1), 7153 (2015).
2. T. Bruegmann, P. M. Boyle, C. C. Vogt, T. V. Karathanos, H. J. Arevalo, B. K. Fleischmann, N. A. Trayanova, and P. Sasse, "Optogenetic defibrillation terminates ventricular arrhythmia in mouse hearts and human simulations," J. Clin. Invest. **126**(10), 3894–3904 (2016).
3. R. C. Wykes, D. M. Kullmann, I. Pavlov, and V. Magloire, "Optogenetic approaches to treat epilepsy," J. Neurosci. Methods **260**, 215–220 (2016).
4. J. C. Williams and T. Denison, "From Optogenetic Technologies to Neuromodulation Therapies," Sci. Transl. Med. **5**(177), 177ps6 (2013).
5. R. R. Allison and K. Moghissi, "Photodynamic therapy (PDT): PDT mechanisms," Clin. Endosc. **46**(1), 24–29 (2013).
6. H. Chung, T. Dai, S. K. Sharma, Y.-Y. Huang, J. D. Carroll, and M. R. Hamblin, "The Nuts and Bolts of Low-level Laser (Light) Therapy," Ann. Biomed. Eng. **40**(2), 516–533 (2012).
7. N. McAlinden, D. Massoubre, E. Richardson, E. Gu, S. Sakata, M. D. Dawson, and K. Mathieson, "Thermal and optical characterization of micro-LED probes for in vivo optogenetic neural stimulation," Opt. Lett. **38**(6), 992 (2013).
8. R. Nazempour, Q. Zhang, R. Fu, and X. Sheng, "Biocompatible and Implantable Optical Fibers and Waveguides for Biomedicine," Materials **11**(8), 1283 (2018).
9. L. Wang, C. Zhong, D. Ke, F. Ye, J. Tu, L. Wang, and Y. Lu, "Ultrasoft and Highly Stretchable Hydrogel Optical Fibers for In Vivo Optogenetic Modulations," Adv. Opt. Mater. **6**(16), 1800427 (2018).
10. M. Choi, M. Humar, S. Kim, and S.-H. Yun, "Step-Index Optical Fiber Made of Biocompatible Hydrogels," Adv. Mater. **27**(27), 4081–4086 (2015).
11. J. Guo, X. Liu, N. Jiang, A. K. Yetisen, H. Yuk, C. Yang, A. Khademhosseini, X. Zhao, and S.-H. Yun, "Highly Stretchable, Strain Sensing Hydrogel Optical Fibers," Adv. Mater. **28**(46), 10244–10249 (2016).
12. M. Hahn, L. Taite, J. Moon, M. Rowland, K. Ruffino, and J. West, "Photolithographic patterning of polyethylene glycol hydrogels," Biomaterials **27**(12), 2519–2524 (2006).
13. A. L. Rutz, K. E. Hyland, A. E. Jakus, W. R. Burghardt, and R. N. Shah, "A Multimaterial Bioink Method for 3D Printing Tunable, Cell-Compatible Hydrogels," Adv. Mater. **27**(9), 1607–1614 (2015).
14. S. Hong, D. Sycks, H. F. Chan, S. Lin, G. P. Lopez, F. Guilak, K. W. Leong, and X. Zhao, "3D Printing of Highly Stretchable and Tough Hydrogels into Complex, Cellularized Structures," Adv. Mater. **27**(27), 4035–4040 (2015).

Optical Materials EXPRESS

15. C. W. Peak, J. J. Wilker, and G. Schmidt, "A review on tough and sticky hydrogels," Colloid Polym. Sci. **291**(9), 2031–2047 (2013).
16. M. B. Browning, S. N. Cereceres, P. T. Luong, and E. M. Cosgriff-Hernandez, "Determination of the in vivo degradation mechanism of PEGDA hydrogels," J. Biomed. Mater. Res., Part A **102**(12), 4244–4251 (2014).
17. M. Choi, J. W. Choi, S. Kim, S. Nizamoglu, S. K. Hahn, and S. H. Yun, "Light-guiding hydrogels for cell-based sensing and optogenetic synthesis in vivo," Nat. Photonics **7**(12), 987–994 (2013).
18. Y. Park, J. Liang, Z. Yang, and V. C. Yang, "Controlled release of clot-dissolving tissue-type plasminogen activator from a poly(l-glutamic acid) semi-interpenetrating polymer network hydrogel," J. Controlled Release **75**(1-2), 37–44 (2001).
19. F. Yang, C. G. Williams, D. Wang, H. Lee, P. N. Manson, and J. Elisseeff, "The effect of incorporating RGD adhesive peptide in polyethylene glycol diacrylate hydrogel on osteogenesis of bone marrow stromal cells," Biomaterials **26**(30), 5991–5998 (2005).
20. N. R. Patel, A. K. Whitehead, J. J. Newman, and M. E. Caldorera-Moore, "Poly(ethylene glycol) Hydrogels with Tailorable Surface and Mechanical Properties for Tissue Engineering Applications," ACS Biomater. Sci. Eng. **3**(8), 1494–1498 (2017).
21. R. Core Team, *R: A Language and Environment for Statistical Computing* (R Foundation for Statistical Computing, 2019).
22. H. Wickham, R. Francois, L. Henry, and K. Müller, "dplyr: A Grammar of Data Manipulation," (2017).
23. H. Wickham, *Ggplot2: Elegant Graphics for Data Analysis* (Springer-Verlag New York, 2009).
24. J. Schindelin, I. Arganda-Carreras, E. Frise, V. Kaynig, M. Longair, T. Pietzsch, S. Preibisch, C. Rueden, S. Saalfeld, B. Schmid, J.-Y. Tinevez, D. J. White, V. Hartenstein, K. Eliceiri, P. Tomancak, and A. Cardona, "Fiji: an open-source platform for biological-image analysis," Nat. Methods **9**(7), 676–682 (2012).
25. Y. Mao, "Nearest Neighbor Distances Calculation with ImageJ," https://icme.hpc.msstate.edu/mediawiki/index.php/Nearest_Neighbor_Distances_Calculation_with_ImageJ.
26. J. A. Killion, L. M. Geever, D. M. Devine, J. E. Kennedy, and C. L. Higginbotham, "Mechanical properties and thermal behaviour of PEGDMA hydrogels for potential bone regeneration application," J. Mech. Behav. Biomed. Mater. **4**(7), 1219–1227 (2011).
27. L. E. Bertassoni, M. Cecconi, V. Manoharan, M. Nikkhah, J. Hjortnaes, A. L. Cristino, G. Barabaschi, D. Demarchi, M. R. Dokmeci, Y. Yang, and A. Khademhosseini, "Hydrogel bioprinted microchannel networks for vascularization of tissue engineering constructs," Lab Chip **14**(13), 2202–2211 (2014).
28. W. Norde, F. G. Gonzalez, and C. A. Haynes, "Protein adsorption on polystyrene latex particles," Polym. Adv. Technol. **6**(7), 518–525 (1995).
29. C. Fournier, M. Leonard, I. Le Coq-Leonard, and E. Dellacherie, "Coating Polystyrene Particles by Adsorption of Hydrophobically Modified Dextran," Langmuir **11**(7), 2344–2347 (1995).
30. J. M. Anderson, A. Rodriguez, and D. T. Chang, "Foreign body reaction to biomaterials," Semin. Immunol. **20**(2), 86–100 (2008).
31. M. B. Browning, T. Wilems, M. Hahn, and E. Cosgriff-Hernandez, "Compositional control of poly(ethylene glycol) hydrogel modulus independent of mesh size," J. Biomed. Mater. Res., Part A **98A**(2), 268–273 (2011).
32. S. Lee, X. Tong, and F. Yang, "The effects of varying poly(ethylene glycol) hydrogel crosslinking density and the crosslinking mechanism on protein accumulation in three-dimensional hydrogels," Acta Biomater. **10**(10), 4167–4174 (2014).
33. V. B. Morris, S. Nimbalkar, M. Younesi, P. McClellan, and O. Akkus, "Mechanical Properties, Cytocompatibility and Manufacturability of Chitosan:PEGDA Hybrid-Gel Scaffolds by Stereolithography," Ann. Biomed. Eng. **45**(1), 286–296 (2017).
34. M. Khandaker, A. Orock, S. Tarantini, J. White, and O. Yasar, "Biomechanical Performances of Networked Polyethylene Glycol Diacrylate: Effect of Photoinitiator Concentration, Temperature, and Incubation Time," Int. J. Biomater. **2016**, 1–8 (2016).